Structure and Fluctuations of Charged Phosphatidylserine Bilayers in the Absence of Salt

Horia I. Petrache,* Stephanie Tristram-Nagle,† Klaus Gawrisch,‡ Daniel Harries,* V. Adrian Parsegian,* and John F. Nagle§

*Laboratory of Physical and Structural Biology, The National Institute of Child Health and Human Development, National Institutes of Health, Bethesda, Maryland; †Department of Biological Sciences, Carnegie Mellon University, Pittsburgh, Pennsylvania; ‡Laboratory of Membrane Biochemistry and Biophysics, The National Institute on Alcohol Abuse and Alcoholism, National Institutes of Health, Rockville, Maryland; and §Department of Physics, Carnegie Mellon University, Pittsburgh, Pennsylvania

ABSTRACT Using x-ray diffraction and NMR spectroscopy, we present structural and material properties of phosphatidylserine (PS) bilayers that may account for the well documented implications of PS headgroups in cell activity. At 30°C, the 18-carbon monounsaturated DOPS in the fluid state has a cross-sectional area of 65.3 Å^2 which is remarkably smaller than the area 72.5 Å^2 of the DOPC analog, despite the extra electrostatic repulsion expected for charged PS headgroups. Similarly, at 20°C, the 14-carbon disaturated DMPS in the gel phase has an area of 40.8 Å^2 vs. 48.1 Å^2 for DMPC. This condensation of area suggests an extra attractive interaction, perhaps hydrogen bonding, between PS headgroups. Unlike zwitterionic lipids, stacks of PS bilayers swell indefinitely as water is added. Data obtained for osmotic pressure versus interbilayer water spacing for fluid phase DOPS are well fit by electrostatic interactions calculated for the Gouy-Chapman regime. It is shown that the electrostatic interactions completely dominate the fluctuational pressure. Nevertheless, the x-ray data definitively exhibit the effects of fluctuations in fluid phase DOPS. From our measurements of fluctuations, we obtain the product of the bilayer bending modulus K_C and the smectic compression modulus B. At the same interbilayer separation, the interbilayer fluctuations are smaller in DOPS than for DOPC, showing that B and/or K_C are larger. Complementing the x-ray data, ^{31}P-chemical shift anisotropy measured by NMR suggest that the DOPS headgroups are less sensitive to osmotic pressure than DOPC headgroups, which is consistent with a larger K_C in DOPS. Quadrupolar splittings for D_2O decay less rapidly with increasing water content for DOPS than for DOPC, indicating greater perturbation of interlamellar water and suggesting a greater interlamellar hydration force in DOPS. Our comparisons between bilayers of PS and PC lipids with the same chains and the same temperature enable us to focus on the effects of these headgroups on bilayer properties.

INTRODUCTION

Although there is an extensive literature on the structure of neutral lipid bilayers, studies of bilayers of lipids with charged headgroups, such as phosphatidylserine (PS) still lag. This lag should be rectified, given the involvement of charged headgroups in cell activity. For example, the exposure of PS in the outer leaflet of the plasma membrane is one of the most striking changes on the surface of apoptotic cells (Fadok et al., 1992; Blankenberg et al., 1998). Ingestion and clearing of apoptotic cells by phagocytes does not occur in the absence of PS (Hoffman et al., 2001). PS serves as a trigger of apolipoprotein J (clusterin) mRNA in the neighboring vital cells of apoptotic cells (Bach et al., 2001). Apoptotic cell death decreases when Neuro 2A cells are enriched with docosahexaenoic acid (DHA, 22:6ω3), and it is thought that the protective effect of DHA is mediated by the accumulation of PS (Kim et al., 2000). In addition to acting at the cellular level, PS lipids have been shown to coactivate (with diacylglycerol) protein kinase C (Takai et al., 1979), an enzyme implicated in signal transduction. Apparently, the chemistry of the PS is important in this molecular triggering event (Johnson et al., 1998), even though alternative proposed mechanisms involve membrane physical properties (Slater et al., 1994; Yang and Glaser, 1995, 1996; Epand et al., 1998). Other recent studies have shown functional roles of PS, not only through direct interaction with membrane proteins (Tsvetkova et al., 2002; Weinreb et al., 2003), but also through regulation of membrane asymmetry (Daleke, 2002; Manno et al., 2002).

From a biophysical perspective, does PS act specifically or nonspecifically? Nonspecific hypotheses implicate the modification of membrane material properties such as compressibility and lateral stress to explain the observed effects of PS on channel activity (Bezrukov et al., 1998) and on the function of membrane receptors (Brown, 1994; Botelho et al., 2002). Indeed, membrane structural properties are known to depend critically on the nature of both acyl chains and the headgroup moiety (Rand and Parsegian, 1989; Gawrisch and Holte, 1996; Nagle and Tristram-Nagle, 2000). It is natural then to expect that structural differences will impact membrane function.

Submitted August 27, 2003, and accepted for publication November 11, 2003.

Address reprint requests to Dr. Horia I. Petrache, National Institutes of Health, Bldg. 9, Rm. 1E116, Bethesda, MD 20892. Tel.: 301-402-7797; E-mail: horia@helix.nih.gov.

Abbreviations used: DLPE, 1,2-dilauroyl-*sn*-glycero-3-phosphoethanolamine; DMPC, 1,2-dimyristoyl-*sn*-glycero-3-phosphocholine; DPPC, 1,2-dipalmitoyl-*sn*-glycero-3-phosphocholine; DPPS, 1,2-dipalmitoyl-*sn*-glycero-3-phospho-L-serine; DOPC, 1,2-dioleoyl-*sn*-glycero-3-phosphocholine; DOPE, 1,2-dioleoyl-*sn*-glycero-3-phosphoethanolamine; DOPS, 1,2-dioleoyl-*sn*-glycero-3-phospho-L-serine; POPS, 1-palmitoyl-2-oleoyl-*sn*-glycero-3-phospho-L-serine; SOPC-d_{35}, 1-stearoyl(d35)-2-oleoyl-*sn*-glycero-3-phosphocholine; SOPS-d_{35}, 1-stearoyl(d35)-2-oleoyl-*sn*-glycero-3-phospho-L-serine.

0006-3495/04/03/1574/13 $2.00

Major differences between neutral phosphatidylcholine (PC) and phosphatidylethanolamine (PE) bilayers are well documented in terms of structural and dynamical parameters (Wilkinson and Nagle, 1981; McIntosh, 1980; Marsh et al., 1983; Rand and Parsegian, 1989; Mason and O'Leary, 1990; Gawrisch and Holte, 1996; Thurmond et al., 1991; Davies et al., 1992; Petrache et al., 2000). PE bilayers are more rigid and more laterally compressed than the PCs. Interbilayer hydration repulsion is qualitatively weaker between PE and PC, a feature relevant to fusion mechanisms (Parsegian and Rand, 1983; Simon et al., 1991).

At neutral pH, phosphatidylserine is charged. How does headgroup charge influence bilayer properties compared to those of PC and PE? Using deuterium and phosphorus NMR, Browning and Seelig (1980) found a relatively rigid structure for the PS headgroup compared to both PC and PE; this was confirmed by de Kroon et al. (1990). By FTIR, Lewis and McElhaney (2000) showed increased PS hydrogen bonding compared to PC. Systematic x-ray studies of the homologous series of saturated PS by Hauser et al. (1982) reported that, whereas infinite swelling of NH_4^+ salts occurs in both the gel and fluid phases, bilayer thickness remains constant. The complex effects of pH, electrostatics, ion binding, and headgroup hydration have been studied by Cevc et al. (1981) and MacDonald et al. (1976) for disaturated phosphatidylserines.

Here we study the monounsaturated dioleoylphosphatidylserine sodium salt ($DOPS^-Na^+$) in water with no added salt (i.e., with its Na^+ counterion only) as in Cowley et al. (1978), Loosley-Milman et al. (1982), and Demé et al. (2002a,b). We use x-ray diffraction, NMR spectroscopy, and density measurements to determine the structure of the fluid phase DOPS lipid bilayers and compare to previous results for the neutral dioleoylphosphatidylcholine, DOPC (Tristram-Nagle et al., 1998). This comparison is of interest since DOPS, DOPC, and DOPE have been used in the membrane protein studies mentioned above. By x-ray diffraction, in addition to average structural parameters, we also obtain information on bilayer fluctuations and material properties of the multilamellar DOPS structure. We learn that DOPS bilayers are thicker than DOPC bilayers, with a correspondingly smaller cross-sectional area. At similar interbilayer separations, bilayer fluctuations are smaller for PS, indicating a more rigid multilamellar structure than for PC. Charged PS, however, swells indefinitely, as opposed to finite swelling limits characteristic of neutral PC and PE. Measured by deuterium-labeled saturated chain probes, DOPS acyl chains appear more ordered than for DOPC, yet laterally compressible under osmotic stress. At the same time, the average orientation of PS headgroups with respect to the bilayer normal is insensitive to water content, shown by NMR ^{31}P-chemical shift anisotropy. Water ordering, however, is more pronounced for DOPS, as expected for a charged headgroup.

X-ray measurements on gel phase DMPS (needed for determination of DOPS structure) allow a parallel PS/PC comparison with the recently determined gel phase structure of DMPC (Tristram-Nagle et al., 2002). Considered in the context of available PC and PE data for both gel and fluid phases, PS reveals properties that could lead to the understanding of complex biological bilayers in terms of material properties of lipid mixtures.

EXPERIMENTAL PROCEDURES

The phospholipids 1,2-dimyristoyl-*sn*-glycero-3-phospho-L-serine (DMPS), 1,2-dioleoyl-*sn*-glycero-3-phospho-L-serine (DOPS), 1,2-dioleoyl-*sn*-glycero-3-phosphocholine (DOPC), 1-stearoyl(d35)-2-oleoyl-*sn*-glycero-3-phospho-L-serine (SOPS-d_{35}), and 1-stearoyl(d35)-2-oleoyl-*sn*-glycero-3-phosphocholine (SOPC-d_{35}) were purchased from Avanti Polar Lipids (Alabaster, AL) and were used without further purification. The label d_{35} denotes a perdeuterated stearic acid chain. All PS lipids were sodium salts. No buffer or added salt was used in any of our experiments.

X-ray scattering from unoriented samples

Polyethyleneglycol (PEG) 35,000 g/mol was first mixed with deionized water and this solution was then mixed with DOPS lipid in 3:1–12:1 weight ratios to give final PEG concentrations (Tristram-Nagle et al., 1998) between 0 and 55 wt %. For each PEG concentration, the osmotic pressure values were calculated by numerical interpolation of the data from Rand et al. (1988, and http://aqueous.labs.brocku.ca). The DOPS/PEG samples were loaded into thin-walled 1.0-mm glass x-ray capillaries and x-ray data were collected at the F3 station of the Cornell High Energy Synchrotron Source (CHESS) using the setup described in Tristram-Nagle et al. (1998).

X-ray scattering from oriented samples

Oriented samples were prepared using the rock-and-roll method (Tristram-Nagle et al., 1993), starting with a solution of 4 mg of DMPS in 100 μl TFE:tol, 4:1, v:v, yielding a well-oriented film $\sim$10-μm thick. After evaporation of the organic solvent, the sample was hydrated from water vapor in a new sample chamber designed to overcome the experimental artifacts that had previously led to the vapor-pressure paradox (Katsaras, 1998). Details of our new chamber will be given in another publication. The first chamber that achieved full hydration from the vapor has been previously described (Katsaras and Watson, 2000). X-ray data were collected at the D1 station at CHESS using a charge-coupled device detector with 1024 $\times$ 1024 pixels of 50 μm (Tate et al., 1995; Barna et al., 1999) as described in Tristram-Nagle et al. (2002).

Analysis of x-ray data

Fluid phase scattering peaks were fit using the modified Caillé theory (Zhang et al., 1994; Nagle et al., 1996). The parameters determined by the fitting program are the Caillé η_1 fluctuation parameter, the mean domain size L, and the fluctuation-corrected (and Lorentz-corrected) ratios of form factors $r_h \equiv |F_h/F_1|$. From η_1, the mean-square fluctuation σ^2 in the water spacing between bilayers is calculated as (Petrache et al., 1998a)

$$\sigma^2 = \eta_1 D^2/\pi^2. \quad (1)$$

Electron density profiles, ρ*(z), were obtained by Fourier reconstruction. For gel phase DMPS they were also obtained by modeling (Tristram-Nagle et al., 2002).

Specific volume measurements

The absolute specific volume v_L of DOPS was determined by the neutral buoyancy method using H_2O/D_2O mixtures (Wiener et al., 1988). The

molecular volume is $V_L = v_L M_W/N_A$, where M_W is the molecular weight, including the Na^+ counterion. Because DMPS is denser than D_2O, the neutral buoyancy method could not be used with this lipid. Instead, V_L of DMPS was estimated as described in Results.

Fluid phase structure: area per lipid

The methods for obtaining structural quantities have been reviewed (Nagle and Tristram-Nagle, 2000). The basic structural quantities consist of averages, such as the lateral area per lipid molecule A, the distance D_{HH} between the peaks in the bilayer electron density profiles, and the locations of various Gibbs dividing surfaces, such as the hydrocarbon thickness $2D_C$ and the Luzzati bilayer thickness D_B (Tardieu et al., 1973). In the Luzzati-Gibbs framework, the bilayer thickness D_B is related to the repeat spacing D through the lipid volume fraction, $D_B = DV_L/(V_L + n_W V_W)$, where n_W represents the number of waters per lipid in the repeat unit cell.

The hydrocarbon chain thickness $2D_C$ is first determined for the DMPS gel phase. The difference in $2D_C$ for the DOPS fluid phase is obtained from differences in D_{HH} measured from electron density profiles obtained from low-angle x-ray diffraction and the equation

$$D_C^{DOPS} = D_C^{DMPS} - (D_{HH}^{DMPS} - D_{HH}^{DOPS})/2. \quad (2)$$

The area A is obtained using

$$A = \frac{V_C}{D_C}, \quad (3)$$

where the hydrocarbon chain volume $V_C = V_L - V_H$ and the headgroup volume is V_H, obtained in Results. The Luzzati bilayer thickness is obtained by $D_B = 2V_L/A$ and the corresponding water thickness is then $D_W = D - D_B$.

^{2}H-NMR experiments on water

All NMR spectra were acquired using a Bruker DMX300 spectrometer equipped with a solids probe with a 5-mm solenoid coil doubly tuned for ^{1}H- and an X-nucleus resonance (Bruker, Billerica, MA). Sample temperature was controlled to within 0.1°C using a Bruker VT control unit. Absolute temperature calibration was accurate to within 0.5°C. The quadrupolar splitting of water was recorded with a 90° pulse followed by data acquisition using CYCLOPS phase cycling and a delay between acquisitions of 2 s. Unoriented DOPC and DOPS dispersions were prepared with D_2O in an argon environment.

Interpretation of water spectra in terms of hydration shells is done following Gawrisch et al. (1985), with the assumptions that 1), distinct shells of water molecules exist with different quadrupolar splittings; 2), the quadrupolar splitting of individual shells are independent of water content; 3), the shells are filled consecutively; and 4), all water molecules exchange rapidly (10^{-5} s) between all shells. E.g., for two layers, the measured quadrupolar splitting $\Delta\nu$ is

$$\Delta\nu = \frac{n_1}{n_W}\Delta\nu_1 + \frac{n_2}{n_W}\Delta\nu_2 = \frac{n_1}{n_W}\Delta\nu_1 + \frac{n_W - n_1}{n_W}\Delta\nu_2$$
$$= \frac{n_1}{n_W}(\Delta\nu_1 - \Delta\nu_2) + \Delta\nu_2, \quad (4)$$

where n_1 and n_2 are the number of waters in each shell and $n_W = n_1 + n_2$ is the total number of waters. The intercept of $\Delta\nu$ vs. $1/n_W$ for $n_W > n_1$ gives the value $\Delta\nu_2$. Isotropic shells then extrapolate to $\Delta\nu = 0$ for $1/n_w \to \infty$.

^{31}P- and ^{2}H-NMR experiments on lipids

^{31}P-NMR spectra were acquired with a Hahn-echo pulse sequence (90°-τ-180°–τ-acquire), a delay time of $\tau = 40$ μs, and a delay between acquisitions of 1 s. The dipolar interaction between phosphorus and proton was suppressed by applying 10 kHz of proton noise decoupling during acquisition, resulting in an increase of sample temperature of <3°C as established by following known phase transitions of lipids.

^{2}H-NMR spectra were acquired with a phase-cycled quadrupolar echo sequence (90°-τ-90°–τ-acquire) with an interpulse delay of $\tau = 50$ μs and a delay between acquisitions of 0.2 s.

Mixed-chain deuterated lipid probes (10 mol %) were used for ^{2}H-NMR of acyl chains. SOPC-d_{35} was used with DOPC and SOPS-d_{35} with DOPS. Lipid mixtures were prepared in chloroform, dried to a thin film by spinning in a stream of argon, and kept under vacuum overnight. The lipid films were hydrated in deionized water and lyophilized. Samples were prepared directly in glass NMR tubes by weighing ~7 mg of dry lipid mixture and appropriate amounts of deuterium-depleted water (Huster et al., 1998).

The acquired powder spectra were dePaked, and order parameter profiles for the stearoyl chains were calculated by standard methods (Holte et al., 1995; Huster et al., 1998). The quadrupolar splitting $\Delta\nu_Q$ is proportional to a geometrical order parameter (S_{CD}) of the C–D bond relative to the bilayer normal, $\Delta\nu_Q = \frac{3}{4}\chi_Q S_{CD}$, with the quadrupolar coupling constant $\chi_Q = e^2Qq/h = 167$ kHz.

RESULTS

X-ray diffraction

Fig. 1 shows the interlamellar repeat spacings (D) for different osmotic pressures for DOPC (Tristram-Nagle et al., 1998) and DOPS in the fluid phase at 30°C. Both of these force curves are essentially exponential at high pressures, consistent with a hydration repulsion regime (Rand and Parsegian, 1989). Below 20 atm (20×10^5 N/m^2) of osmotic pressure (log [P_{osm}/($dyn\ cm^{-2}$)] = 7.3), DOPS deviates significantly from DOPC. At zero osmotic pressure, DOPC reaches a finite swelling limit, $D = 63.1$ Å, whereas DOPS apparently swells indefinitely. With unoriented samples we

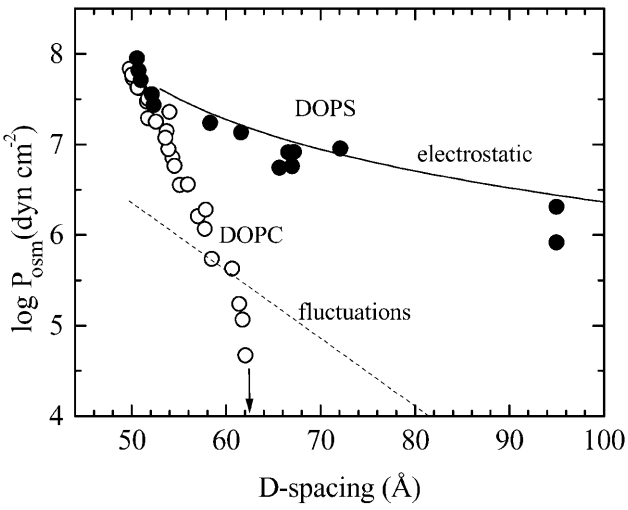

FIGURE 1 Force curves of fluid multilamellar DOPS (●) and DOPC (○) bilayers at 30°C. At zero osmotic pressure, D for DOPC reaches the limit indicated by the arrow. The dashed line shows the undulation pressure for DOPC from Tristram-Nagle et al. (1998). The electrostatic pressure according to Eq. 7 is shown by a solid line using measured bilayer thickness $D_B = 38.3$ Å.

have measured D-spacings up to 100 Å (at 1 atm), but even larger values have been observed at lower osmotic pressures (Demé et al., 2002a,b).

Fig. 2 shows representative x-ray scattering peak shapes taken with high instrumental resolution. Three diffraction peaks are observed for this particular DOPS sample, which is typical for fluctuating lipid bilayers under mild osmotic stress (Nagle et al., 1996; Tristram-Nagle et al., 1998; Demé et al., 2002a,b). Four or more peaks are seen under high osmotic pressure and only two peaks are observable at low pressures. The scattering peaks are well fit by the modified Caillé theory (MCT) (Zhang et al., 1994) for $P_{osm} > 3$ atm, where the usual harmonic constraint $\eta_h = h^2\eta_1$ was imposed for all orders h. At smaller pressures the scattering peaks were too weak to allow reliable fits. From the fits, we determine the D shown in Fig. 1, form factor ratios, F_h/F_1, and the Caillé fluctuation parameter, η_1, from which the root-mean square fluctuation in water spacing, σ, is determined by Eq. 1. Fig. 3 *A* shows σ vs. D. Comparison to results for DOPC shows that fluctuations increase with repeat spacing D for both lipids. At the same D-spacing, fluctuations are smaller for DOPS than for DOPC. In contrast, Fig. 3 *B* shows that there are larger fluctuations in DOPS than DOPC at the same osmotic pressure; this reversal is allowed by the much different force-distance relations shown in Fig. 1.

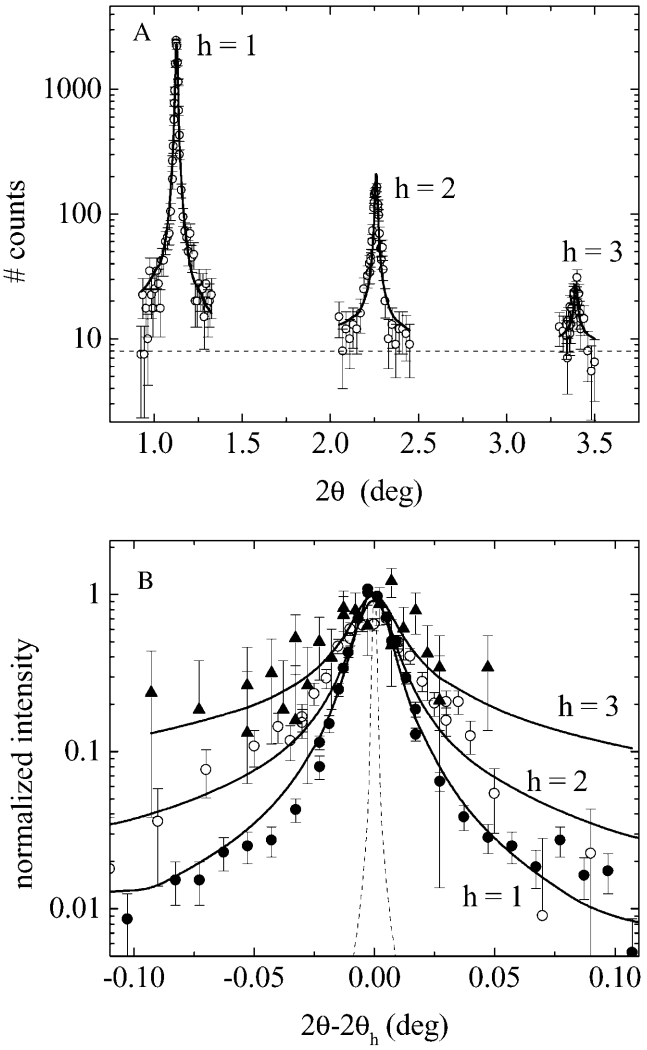

FIGURE 2 Representative fit (*solid lines*) to high-resolution x-ray diffraction spectra (*symbols*) of multilamellar DOPS vesicles at 30°C in the presence of 25% PEG ($\log P_{osm} = 6.97$). (*A*) Data shown as a function of the absolute scattering angle 2θ. Dashed line shows the background level. (*B*) Peaks are scaled and superimposed to emphasize that the tails grow with order number, consistent with the MCT theory shown with solid lines. The dashed curve shows the instrumental resolution function.

NMR spectroscopy

Fig. 4 *A* shows that there is a marked difference in the ^{31}P-chemical shift anisotropy in DOPS compared to DOPC. For DOPC, the anisotropy increases with increasing numbers of water molecules per lipid n_W (Gally et al., 1975; Gawrisch

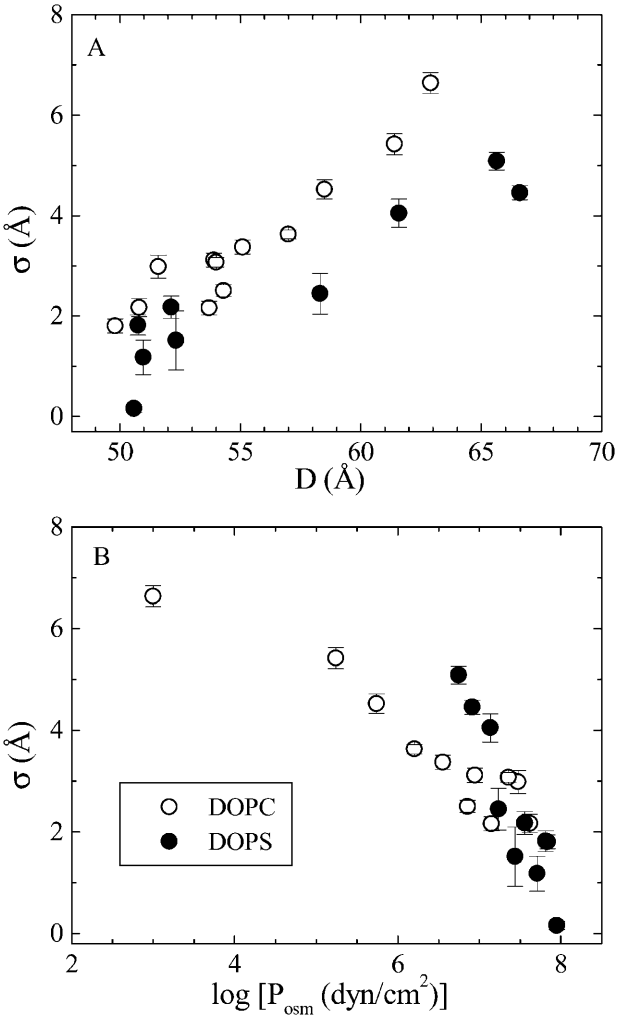

FIGURE 3 Interlamellar spacing fluctuations σ (Eq. 1) as a function of (*A*) interlamellar repeat spacing D and (*B*) as a function of osmotic pressure P_{osm} for DOPC (Tristram-Nagle et al., 1998) and DOPS.

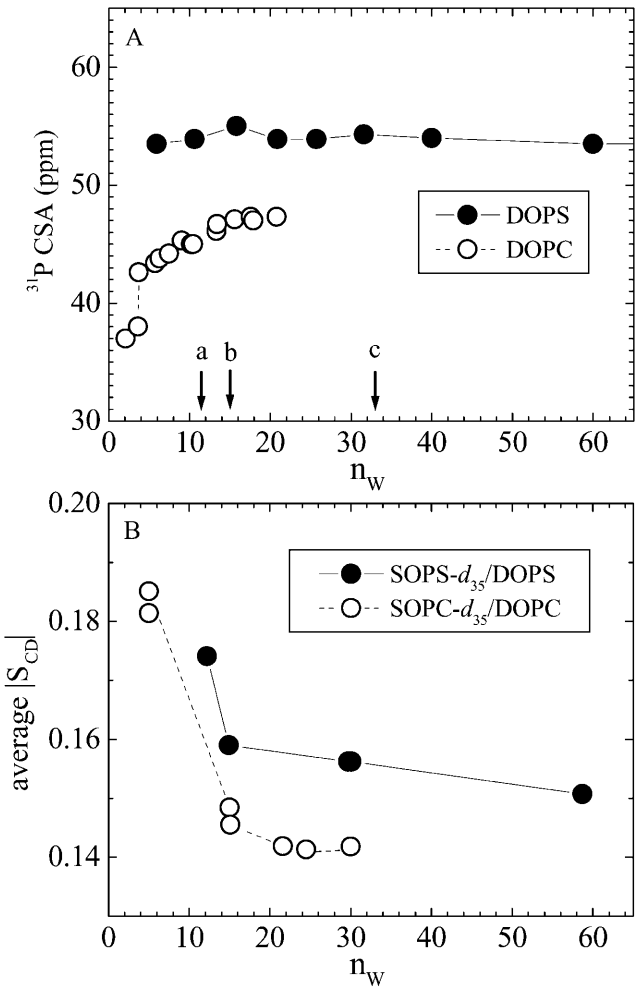

FIGURE 4 (*A*) Chemical shift anisotropy of lipid phosphorus atom versus the number of waters per lipid (n_W). The arrows in *A* indicate reference hydration levels for DOPC (Tristram-Nagle et al., 1998): a, all waters are in the headgroup region $n_W = 11(= n'_W)$; b, $n_W = 14.5$ interlamellar waters at $P = 56$ atm osmotic pressure; and c, $n_W = 32.5$ interlamellar waters at full hydration $P = 0$. (*B*) Average order parameters of deuterated stearoyl probes versus n_W. All data at 30°C except DOPS data in *A* at 22°C.

et al., 1985). By contrast, ^{31}P-chemical shift anisotropy of DOPS is larger in magnitude and is insensitive to changes in water content (measured by us up to 250 waters/DOPS), as previously shown by Browning and Seelig (1980).

To measure the effect of hydration on chain packing we have used mixed-chain deuterated lipid labels as reporters (Separovic and Gawrisch, 1996), SOPC-d_{35} in host DOPC and SOPS-d_{35} in host DOPS, and we measured the order parameter profiles for the deuterated saturated stearoyl chains in the reporter lipids. The average order parameters, shown in Fig. 4 *B*, give a measure of hydrocarbon chain packing variation with water content (Separovic and Gawrisch, 1996; Koenig et al., 1997). Since the order parameters for pure SOPC-d_{35} and SOPS-d_{35} are much larger in magnitude (Huster et al., 1998), the values in Fig. 4 *B* reflect the effect of the host bilayers. The acyl chain order decreases with increasing hydration. The order parameters are larger for DOPS, indicating a smaller area per lipid for the PS headgroup. Significant changes are seen at small water content (<15 waters per lipid) when apposing bilayers come into close contact. Smaller variations are seen at higher water content.

The effect of lipid headgroup on the interlamellar water is shown in Fig. 5 in terms of deuterium quadrupolar splittings (heavy water was used in these measurements). The ^{2}H-NMR spectra (not shown) indicate homogeneous mixing with resolvable splittings at 30 waters per lipid or less for DOPS. For DOPC there is an excess water phase for $n_W >$ 32.5. At high water content, isotropic peaks dominate and quadrupolar splittings cannot be resolved. The lowest splitting resolved was ~0.6 kHz. Except at very small water

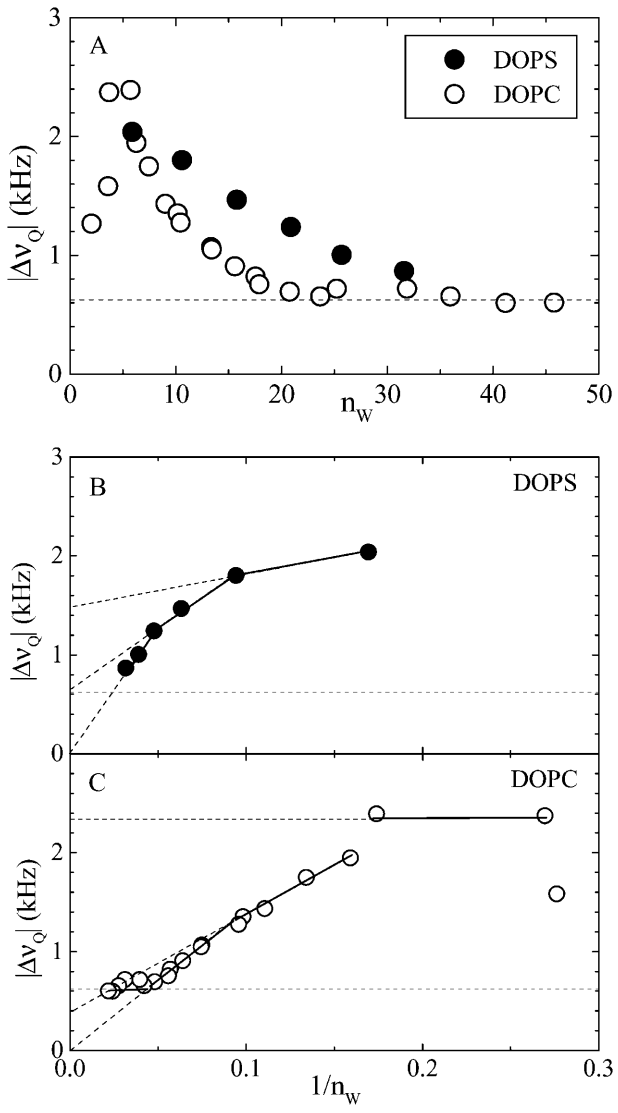

FIGURE 5 Quadrupolar splitting of water deuterium versus (*A*) the number of waters per lipid n_W and versus $1/n_W$ for (*B*) DOPS at 22°C and (*C*) DOPC at 30°C. Horizontal dashed lines show the limit of resolution.

content, the average water quadrupolar splitting is larger for DOPS than for DOPC, so the PS headgroups, together with their counterions, exert a stronger perturbation on the interlamellar water than the zwitterionic PC.

Plotted versus the inverse number of waters per lipid, $1/n_W$ (Fig. 5, *B* and *C*), the quadrupolar splittings can be interpreted in terms of hydration shells (Gawrisch et al., 1985; Volke et al., 1994a,b). The intercepts of linear extrapolations correspond to the average splittings of individual shells. Even though the changes seen in Fig. 5 with n_W are continuous, formal decomposition into discrete shells facilitates comparison between the two lipids. For DOPS, a first (inner) shell next to the headgroups consists of highly perturbed water molecules ($n_1 = 11$) with a quadrupolar splitting of $\Delta\nu_1 = 1.5$ kHz. Between this and an outer isotropic shell, an intermediate shell exists with $n_2 = 10$ and $\Delta\nu_1 = 0.6$ kHz. For DOPC, the inner and the intermediate shells each consists of approximately six waters, with $\Delta\nu_1 = 2.3$ kHz and $\Delta\nu_2 = 0.4$ kHz. The quadrupolar splitting becomes constant at $n_W = 24$ or more. All values are approximate within ± 1 water molecules.

Structural results

Numerical values for structural results are given in Table 1. The first important number is area *A* for gel phase DMPS. This is obtained directly from wide-angle x-ray data which consists of a single peak with a scattering *q*-vector in the plane of the bilayer. This indicates hexagonal packing of chains oriented perpendicular to the DMPS bilayer. Because there is no chain tilt, the area per lipid is simply twice the cross-sectional area per chain, $2A_C$. Using the standard formula $A_C = 2d^2/\sqrt{3}$ for hexagonally packed chains (Tardieu et al., 1973; Tristram-Nagle et al., 1993), our measured $d = 4.18$ Å gives $A^{DMPS} = 40.8$ Å^2. It is interesting to compare this cross-sectional chain area $2A_C$ of DMPS with DMPC, for which $2A_C = A \cos\theta_{tilt}$. Although DMPC is not in the gel phase at $T = 20$°C, extrapolation to this temperature using results from Sun et al. (1996) and Tristram-Nagle et al. (2002) yields $2A_C = 40.7$ Å^2. Comparison with $2A_C$ for DMPS shows that the density of chain packing in these gel phases is not significantly affected by the headgroups, which, instead, primarily affect the chain tilt.

TABLE 1 Summary of structural parameters

	DOPC fluid	DOPS* fluid	DMPC gel†	DMPC fluid‡	DMPS gel
T (°C)	30	30	20	30	20
M_W (g/mol)	786.2	810.0	678.0	678.0	701.8
$n_L^*(e)$	434	442	374	374	382
$F(0)(e/Å^2)$	0.0	1.03	0.9	0.2	2.85
v_L (ml/g)	0.998	0.913	0.93	0.978	0.84
V_L (Å^3)	1303	1228	1050	1101	979
V_H (Å^3)	319	244	319	319	244
V_C (Å^3)	984	984	731	782	734
D (Å)	63.1	52.5 (∞)	59.9	62.7	∞
D_{HH} (Å)	36.9	39.0 (38.4)	40.1	36.0	44.3
D_C (Å)	13.6	15.4 (15.1)	15.2	13.1	18.0
D_B (Å)	36.0	38.3 (37.6)	43.7	36.9	47.8
A (Å^2)	72.5	64.1 (65.3)	48.1	59.7	40.8

*Structural parameters at zero osmotic pressure obtained by extrapolation are shown in parentheses.

†From gel data at 10°C that has been extrapolated to 20°C (Tristram-Nagle et al., 2002).

‡Data from Petrache et al. (1998b).

The intensities of low-angle lamellar diffraction peaks for gel phase DMPS were obtained from oriented samples that had up to $h = 11$ orders of diffraction. The absolute value of the bilayer form factors $|F(q = 2\pi h/D)|$ that were obtained from the intensities are shown in Fig. 6 *A* for orders $h = 1$–4 for five different hydration levels (different *D*-spacings). The 0^{th} order $F(0)$ was obtained using volumetric data and the fundamental relation $AF(0) = 2(n_L^* - \rho_W^* V_L)$ (Nagle and Wiener, 1989), where n_L^* is the number of electrons in the lipid and ρ_W^* is the electron density of water. The solid line in Fig. 6 *A* shows the continuous Fourier transform of the

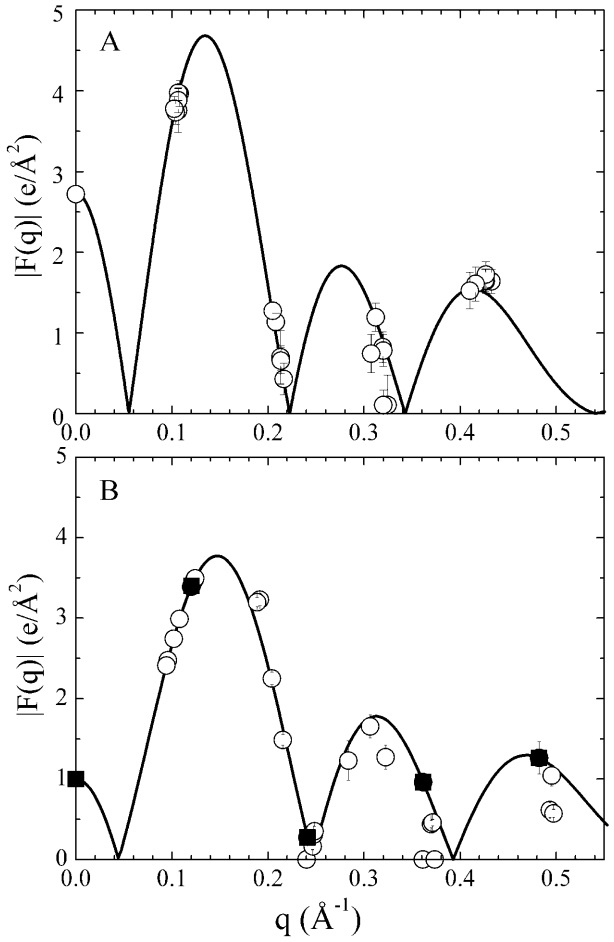

FIGURE 6 Low-angle lamellar data for the form factor $|F(q)|$ is shown by symbols. (*A*) Gel phase DMPS, orders $h = 1$–4 only. The solid line is the best model fit. (*B*) Fluid phase DOPS. The solid line is derived from one sample with data shown with solid squares and $D = 52.5$ Å.

electron density for the best model that was fit to both low-angle and wide-angle x-ray data, using the fitting program developed to analyze DMPC gel phase data (Tristram-Nagle et al., 2002). The result for the half-thickness of the hydrocarbon chain region is $D_C = 18.0$ Å. Then the volume of the hydrocarbon chain region is $V_C^{DMPS} = AD_C = 734$ Å^3. Use of the model method obtains absolute scales for both the continuous transform in Fig. 6 *A* and the electron density profiles shown in Fig. 7 *A*. There are two electron density profiles for DMPS in Fig. 7 *A*. The one labeled $h = 4$ was obtained using only the four orders shown in Fig. 6 *A*. The one labeled $h = 11$ used higher orders (not shown in Fig. 6 *A*). The inclusion of higher orders shows additional structure in the electron density profile in the headgroup region near $z = 20$ Å in Fig. 6 *A*. However, it is important for this study to show the electron density profiles at low spatial resolution ($h = 4$) to obtain a comparison of D_{HH} with the fluid phase of DOPS, for which higher orders of diffraction are unobservable due to fluctuations.

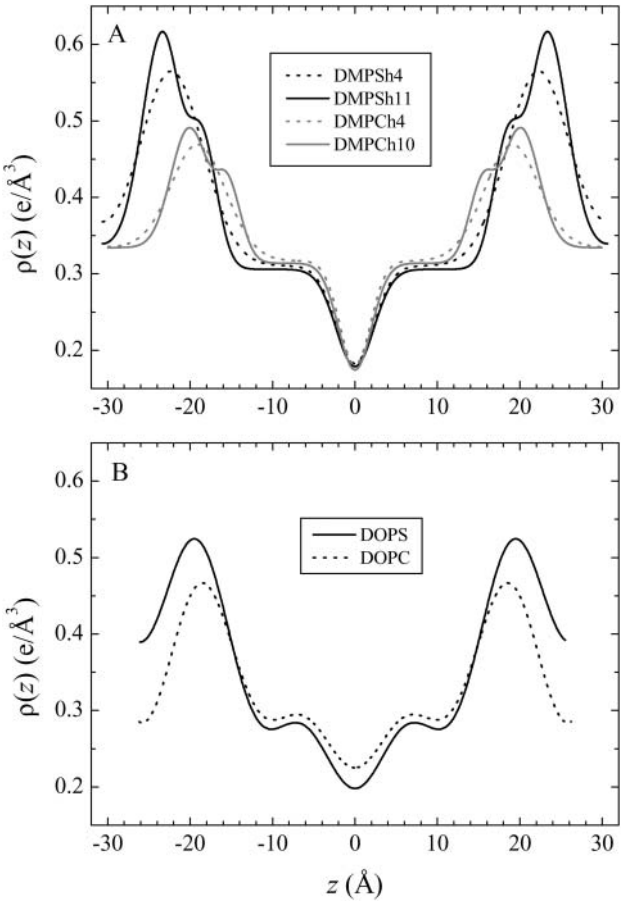

FIGURE 7 Electron density profiles versus normal to the bilayer z. (*A*) Gel phase DMPS at 20°C (*black*) and DMPC at 10°C (*gray*) obtained from model fitting using four (*dashed*) or more (*solid*) orders of diffraction. (*B*) Fluid phase DOPS (*solid*) and DOPC (*dashed*) at 30°C, both constructed using Fourier series with four orders of diffraction.

The electron density profile for DMPS in the gel phase is compared to DMPC in Fig. 7 *A*. The larger bilayer thickness of DMPS is expected because the chains are not tilted in DMPS whereas they are tilted by >30° in DMPC (Tristram-Nagle et al., 2002). The density in the methylene plateau region is similar for the two lipids. The larger methyl trough in the case of DMPS is expected because the area A is smaller, so there is a larger effective density of methyl groups along the bilayer normal. The headgroup peaks are larger for DMPS than for DMPC. This is due to an overall larger electron density in PS headgroups. Whereas the number of electrons in a PS headgroup (including the Na^+ ion) is larger by only 5% (172 *e* vs. 164 *e*), headgroup volume is smaller by almost 30% (Table 1 and see below). The shape of the headgroup peak is similar for DMPS and DMPC; in the high-resolution profiles ($h = 11$) there is a marked shoulder toward the hydrocarbon region due to the carbonyl groups.

Moving on now to fluid phase DOPS, the neutral buoyancy measurements obtained $V_L^{DOPS} = 1228.2$ Å^3 at 30°C, which is smaller than the volume of DOPC by 75 Å^3. From previous results for fluid phase lipids (Nagle and Tristram-Nagle, 2000), it is reasonable to consider the approximation that the volumes of the oleoyl chains are the same in fluid phase DOPC and DOPS. Headgroup volume for PCs has been given as $V_H^{PC} = 319$ Å^3 (Tristram-Nagle et al., 2002). Subtracting the measured difference in total volumes then gives $V_H^{PS} = 244$ Å^3 for the PS headgroup. Adding this to the measured V_C of DMPS gel phase gives the value of V_L for the gel phase in Table 1.

The low-angle x-ray intensities for fluid phase DOPS were obtained from unoriented MLV samples for which only $h = 4$ orders could be obtained. The resulting form factors obtained from MCT analysis are shown in Fig. 6 *B*. To obtain the continuous transform shown there, the usual sampling theorem was applied to the data from one sample with one D-spacing. The area A of the fluid phase was obtained using Eqs. 2 and 3. The head-to-head spacing D_{HH}^{DOPS} was obtained as the average from the Fourier reconstruction of the $h = 1$–4 electron density profiles of fluid phase DOPS, shown in Fig. 7 *B*. The D_{HH}^{DMPS} was also obtained from the Fourier reconstruction of the $h = 1$–4 electron density profiles of gel phase DMPS; this value of D_{HH}^{DMPS} was negligibly different from the modeling result ($h = 4$) shown in Fig. 7 *A*. The electron density of DOPS was put on an absolute scale by requiring the integrated size of the headgroup peaks to be consistent with the number of electrons in the headgroup as previously described (Petrache et al., 1998b; Tristram-Nagle et al., 1998). The results for the structural parameters for DOPS are listed in Table 1. Comparing fluid phase profiles of DOPS and DOPC in Fig. 7 *B*, we again observe larger headgroup densities for DOPS, as occurred in Fig. 7 *A* for the gel phase DMPS lipid. The area $A^{DOPS} = 64.1$ Å^2 is significantly smaller than $A^{DOPC} = 72.5$ Å^2 and this is consistent with the larger D_{HH} seen from

electron density profiles (Fig. 7 *B*). A larger area for DOPC is also consistent with the order parameters measured by ^{2}H-NMR shown in Fig. 4 *B*. However, the area difference estimated from these order parameters (see Koenig et al., 1997) appears significantly smaller, of ~2–3% instead of >10% obtained from x-ray.

DISCUSSION

Structure

Of our structural results in Table 1, a striking result is that areas *A* of phosphatidylserine lipids are considerably smaller in both gel and fluid phases than the corresponding phosphatidylcholine lipids that have the same chains at the same temperature. We will call this the *condensing effect*. For gel phase DMPS, the condensing effect is accompanied by having untilted chains, compared to benchmark DMPC and DPPC for which chains are tilted by >30° with respect to the bilayer normal. Chain tilting costs little free energy compared to changes in hydrocarbon density; indeed, we found that the hydrocarbon chain density is very nearly the same in DMPC and DMPS. As emphasized previously (Sun et al., 1996) tilting is an easy degree of freedom that all-*trans* gel phase hydrocarbon chains possess that allows them to accommodate to constraints imposed by headgroup interactions. The fact that gel phase PS chains do not tilt whereas PC chains do, is a reflection, then, of the PS heads requiring less area *A* than PC heads.

The condensing effect of PS lipids is not what one might have expected, because the net charge on PS lipids provides an additional electrostatic repulsion that would tend to make *A* larger than for the PC lipid with the same chains. Of course, electrostatic repulsion could be reduced if the Na^+ counterions were bound between the headgroups. It has been estimated from molecular dynamics simulations that more than one-half of the Na^+ counterions might be considered to be included within the membrane when the membrane surface is defined to be at the distance of the serine carboxyl from the bilayer center (Pandit and Berkowitz, 2002; Mukhopadhyay et al., 2004). Nevertheless, this would only reduce the electrostatic repulsion, not reverse its sign. This is consistent with the expectation that there is a net surface charge on PS bilayers to bring about the unlimited increase in *D* with increasing water content. It therefore appears that there is some other cause of the condensing effect.

There is one aspect of the measurements that brings about a condensing effect in DOPS compared to DOPC. To measure the area of 64.1 Å^2 in DOPS, it was necessary to impose an osmotic pressure P_{osm}, and this is well known to compress the bilayer laterally. The relaxed A_0 can be calculated from (Rand and Parsegian, 1989; Nagle and Tristram-Nagle, 2000),

$$A_0 = A(1 + PD_W/K_A). \quad (5)$$

For the DOPS sample used in Fig. 7, $D = 50.3$ Å, $P = 40$ atm, and $D_W = 12.3$ Å. Because the lateral area compressibility K_A has not been measured for DOPS, we use $K_A = 265\ dyn/cm = 0.265\ N/m$ for DOPC (Rawicz et al., 2000), which was measured in the pressure range used here and should be a lower bound to K_A for DOPS. This yields $A_0 = 65.3$ Å^2 for DOPS with no osmotic pressure, which falls short of the measured $A_0 = 72.5$ Å^2 for DOPC by 7.2 Å^2. K_A would have to be almost one order-of-magnitude smaller to fully account for the difference. Such small K_A, however, is ruled out by the probe measurements in Fig. 4 *B*. The osmotic pressure in the DOPS experiment cannot account for the condensing effect.

It is worth noting that DOPC area is one of the largest values measured for fluid PC lipids, suggesting that the oleoyl chains take PC lateral separation to an extreme. From this perspective, PS headgroups must work against the disordering tendency of the unsaturated chains. It is of interest to use K_A of DOPC to estimate how much work is required to compress the oleoyl chains down to the DOPS area, by calculating the free energy of compression (Parsegian et al., 1979),

$$\Delta G = (1/2)K_A(\Delta A/A)\Delta A, \quad (6)$$

where $\Delta A = A_0^{DOPC} - A_0^{DOPS} = 7.2$ Å^2. This gives a modest 0.3 k_BT per lipid, which indicates how easily the area of fluid unsaturated chains can accommodate to headgroup preferences.

Of course, the condensing effect ΔA could be caused either by an attractive lateral force on the PS headgroups or by a repulsive force on the PC headgroups. The tilting of the hydrocarbon chains in gel phase DMPC compared to no tilt in DMPS implies that the PC headgroup has a larger steric radius than the PS headgroup, even though this is not obvious when one compares the steric van der Waals radii of the two headgroups. However, steric forces are quite short-range, so they are unlikely to play a significant role for DOPC whose *A* is >50% larger in its fluid phase than its gel phase counterparts, DMPC and DPPC. Perhaps more importantly, PS headgroups at neutral pH have three centers, a PO_4^-, a COO^-, and an NH_3^+, which can form hydrogen bonds to adjacent lipids. Such hydrogen bonding has been suggested to account for the condensing effect and the higher phase transition temperatures of phosphatidylethanolamine (PE) lipids (Nagle, 1976), where it was emphasized that the bonds would be weak and transient, consistent with retaining appreciable lateral mobility and consistent with the small free energy of compression required of the PS headgroups calculated above. Indeed, the hydrogen-bonding propensity of PS lipids has been measured using FTIR (Lewis and McElhaney, 2000). Formation of hydrogen bonds and lateral compression from DPPC to DPPS has been emphasized in molecular dynamics simulations (Pandit and Berkowitz, 2002), where it was found that lateral condensation involves the formation of hydrogen bonds between the NH_3^+ and the

PO_4^- groups as well as binding of Na^+ to the COO^- group. An equivalent way to think about the condensing effect is that hydrogen bonds reduce the distance at which steric interactions become important when compared to the sum of van der Waals radii. This qualitatively explains why the effective volume of the headgroup V_H in Table 1 is so small compared to the PC headgroup even though the PS headgroup has an extra carboxyl to partially compensate for the loss of the choline methyls. Indeed, our results in Table 1 indicate that V_H is 30% smaller for PS than for PC headgroups. Imagining the crudest model of headgroups as spheres, this would provide a difference in A of 20%, which coincides nicely with the ratio of the areas A^{DMPC}/A^{DMPS} in the gel phase where steric interactions between headgroups play the dominant role for A.

The change in lateral density seen from changing PC to PS headgroups is strikingly similar to the change seen from demethylating PC headgroups (giving a PE). Even though the PS headgroup has an extra carboxyl group and the Na^+ counterion, the PS and PE headgroup volumes are similar. This is seen by comparing the V_H values in Table 1 with the value 246 $Å^3$ that can be deduced for DLPE from Table 6 of Nagle and Tristram-Nagle (2000). An electrostrictive effect on water due to the net charge on the PS headgroup would reduce the apparent V_H below that estimated from van der Waals radii of the headgroup. An electrostrictive effect on water is also consistent with the larger $\Delta\nu_Q$ that we observe in the D_2O NMR data in Fig. 5. It may also be noted that a substantially larger V_H for DOPS would lead to the inconsistency that $V_C = V_L - V_H$ would be smaller than the corresponding values obtained for fluid phase hydrocarbon chains in PC lipids and even smaller than values for fluid phase DLPE (Nagle and Tristram-Nagle, 2000).

The similarities between PS and PE lipids may explain previous biological observations. It has been shown that alamethicin channel formation can be controlled in the same fashion by either increasing the concentration of DOPE in DOPC/DOPE mixtures or by lowering the pH of pure DOPS membranes (Bezrukov et al., 1998). Similarly, the rhodopsin photocycle can be modulated by the PS and PE content (Botelho et al., 2002). In both studies, the proposed mechanism for lipid influence on protein function involves the concept of intrinsic curvature and lateral stress (Gruner, 1985) in addition to the effect of electrostatic surface potential. Here we show that the PS headgroups act to compress the bilayers laterally, just as PE does in PE/PC mixtures (Rand and Parsegian, 1989).

Interactions

The standard interactions between adjacent neutral bilayers consist of a short range repulsive hydration interaction and a longer range attractive van der Waals interaction (Cowley et al., 1978). In gel phases, the competition between these bare forces stabilizes the water spacing, D_W, even without an added osmotic pressure, P_{osm}. In fluid phases like DOPC there is an additional repulsion entropically driven by the frustrated thermal fluctuations within the potential profile generated by the bare interactions. This effective fluctuation interaction is longer range than the hydration repulsion and is the dominant repulsion that drives D_W to larger values for fluid phases (Evans and Parsegian, 1986; McIntosh and Simon, 1986; Podgornik and Parsegian, 1992). The dashed line in Fig. 1 shows the fluctuation pressure obtained for DOPC (Tristram-Nagle et al., 1998). This should be an upper bound for the fluctuation pressure of DOPS, which has smaller fluctuations as shown in Fig. 3. It is clear that fluctuation repulsion is far too small to account for the force-distance data for DOPS in Fig. 1.

The obvious force responsible for DOPS swelling is the electrostatic repulsion. The appropriate theoretical equation is (Andelman, 1995),

$$P_{elec}(a) = \frac{\pi k_B T}{2 l_B a^2}, \tag{7}$$

where a is the thickness of the interlamellar water layer and $l_B = e^2/\varepsilon_W k_B T$ is the Bjerrum length, 7.4 Å at 30°C. This equation is based on Poisson-Boltzmann theory for a model of two charged, smooth flat walls in the absence of added salt (counterions only). It also assumes that the system is in the Gouy-Chapman regime of high surface charge which requires $a/b \gg 1$, where b is the Gouy-Chapman length $e/2\pi l_B \sigma_C = A/2\pi l_B$. For one electronic charge per lipid, the value of b is 1.4 Å, which puts DOPS firmly into the Gouy-Chapman regime. Of course, bilayer surfaces are not smooth and this leads us into the issue of where to best place the membrane surface so that a can be calculated from the measured D-spacing (also discussed by Loosley-Millman et al., 1982). The simplest choice is $a = D_W = D - D_B$. From Table 1, D_B is close to the headgroup peak D_{HH} which, in turn, is essentially the location of the electron-dense phosphate group. This choice therefore suggests that the corresponding model represented by Eq. 7 consists of a plane of charged phosphate groups and that the serine group is electrically complacent because it is zwitterionic. In this picture the Na^+ counterion is distributed primarily with values of $z > D_B$. This picture is reasonably consistent with simulations on DPPS (Pandit and Berkowitz, 2002), although the Na^+ and phosphate distribution functions have appreciable overlap due to fluctuations. This picture is also consistent with a simulation on POPS (Mukhopadhyay et al., 2004) in which the bound Na^+ counterions are located deeper in the bilayer near the carbonyl groups. The theoretical pressure resulting from this choice comes reasonably close to fitting the force-distance data as is shown in Fig. 1. It is therefore clear that electrostatic repulsion is the dominant interaction between DOPS bilayers when D exceeds 60 Å. The a^{-2} form of the interbilayer electrostatic interaction is consistent with most of the Na^+ ions being located in the lipid headgroup region. The

predominance of Na-headgroup associations would also be consistent with reduced lateral repulsion between the charged headgroups.

A low-resolution x-ray study of another charged headgroup, phosphatidylglycerol, by Cowley et al. (1978), showed remarkably similar features. They found reduced area per lipid compared to PC as well as charge-independent pressure curves characteristic of the Gouy-Chapman regime. Quantitative interpretation of the pressure curves indicated that only half of the headgroups were charged, suggesting association with protons or perhaps Na^+ counterions, including the possibility that Na^+ ions percolate behind the charged headgroups.

The amplitude of fluctuations σ that we obtain from our high-resolution x-ray data involves two material properties of general interest, the bending modulus K_C and the compression modulus B, through the relation (Petrache et al., 1998a) of

$$\sigma^2(D) = \frac{k_B T}{2\pi} \frac{1}{\sqrt{K_C B}}. \quad (8)$$

For neutral bilayers, K_C is supposed to be a property of individual bilayers and not to depend upon water spacing, and B incorporates the interbilayer interactions. However, electrostatic interactions between bilayers are known to increase the value of K_C in the Gouy-Chapman regime. This increase has been estimated to be $\Delta K_C \approx 0.06\, k_B T (a/l_B)$ (Eq. 7.14 in Andelman, 1995). For our data in Fig. 1 the maximum ΔK_C is $<0.7\, k_B T$. This is small compared to $K_C = 20\, k_B T$ for DOPC (Rawicz et al., 2000). Therefore, electrostatic interactions between bilayers are not likely to cause a significant increase in K_C.

Our data for DOPS have smaller interbilayer fluctuations σ than DOPC at the same D-spacing as shown in Fig. 3. Because the magnitude of $K_C B$ is proportional to the inverse fourth power of σ in Eq. 8, the σ-data require that the $K_C B$ product is larger by an order of magnitude for DOPS when D exceeds 55 Å. It is often assumed that K_C is proportional to the square of the hydrocarbon thickness, D_C^2 (Rawicz et al., 2000), but that would only increase K_C for DOPS by a factor of 1.3 compared to DOPC. This small difference in K_C would suggest that it is the compression parameter B that increases significantly for DOPS for the larger D-spacings, consistent with the interpretation of Fig. 1 that the electrostatic interaction increases the magnitude of the forces that are included in the B parameter.

Indirect evidence for a larger K_C comes from NMR. The ^{31}P-chemical shift anisotropy does not depend on water content for DOPS, but has a strong dependence for DOPC. This suggests a reorientation of the headgroup with increasing water content for DOPC and not for DOPS. This is consistent with a more rigid DOPS membrane, even though it is not the only possible explanation. Likely causes for a larger K_C and more rigidity in PS lipids would be the electrostatic interactions and binding of ions within the headgroup region as well as putative hydrogen bonding. Yet, DOPS bilayers are osmotically compressible, as indicated by the probe measurements in Fig. 4 *B*. Whereas quantitative analysis of these measurements is model-dependent (the probe response depends on its own compressibility), compressibilities on the order of 200–300 dyn/cm can be estimated, which is a typical range for PC bilayers (Rawicz et al., 2000).

As measured by the larger deuterium quadrupolar splittings for the same n_W (Fig. 5), interlamellar water ordering is more pronounced for DOPS than for DOPC. Since A is smaller for DOPS, this implies that water perturbation extends further from the bilayer compared to DOPC. The measured splittings correspond to an orientational order parameter of water molecules with respect to the membrane normal, averaged over all interlamellar water. Different locations along the bilayer normal can be thought to contribute to the overall average according to a local order parameter (Gawrisch et al., 1985; Volke et al., 1994a). Plotted versus the inverse number of waters per lipid ($1/n_W$) (see Fig. 5 *B*), the quadrupolar splittings show a strongly perturbed hydration shell next to the headgroups; an intermediate, less perturbed shell; and finally an isotropic water shell ($\Delta\nu_3 = 0$). These shell structures should be thought of as short-lived snapshots, with lifetimes <1 ns, as all water molecules exchange rapidly between all regions. Adopting this shell description, we find that 11 waters are strongly associated with the PS headgroup and that it takes $\sim$21 waters to reach the linear regime that extrapolates to $\Delta\nu = 0$ in Fig. 5. This is in contrast to DOPC, for which the linear regime is reached earlier, at $\sim$12 waters per PC headgroup, in good agreement with $n'_W = 11$ obtained from x ray (Tristram-Nagle et al., 1998). The hydration force is therefore expected to be different between the two headgroup types (Marsh, 1989; Volke et al., 1994b; Cevc et al., 1995), in accord with the steeper pressure curve for DOPS at small D-spacings. However, because of the short range of this force, it would only affect the B parameter for the smaller interbilayer spacings in Fig. 1.

Small water spacings can facilitate formation of hydrogen bonding between the apposing headgroups of neighboring bilayers, and further modify net interbilayer interactions in this regime. It has been suggested by Rand et al. (1988) and further discussed by McIntosh and Simon (1996) that interlamellar hydrogen bonding could account for the reduced swelling of PE bilayers compared to PC. Interlamellar hydrogen bonding opposes unbinding, but clearly does not prevent it, as seen here for PS. McIntosh and Simon (1996) found that replacing only 25% of the PE heads with charged phosphatidic acid heads brought about unbinding, even with added 100 mM NaCl. This suggests that the sum of the repulsive hydration and electrostatic forces can dominate the interbilayer hydrogen bonding in charged bilayers, and unbinding of the multilamellar stack occurs. In contrast, the overwhelming free energy penalty of exposing

hydrocarbon chains to water maintains in-plane headgroup separation small enough so that short range intrabilayer hydrogen bonding can provide a lateral condensation compared to PC headgroups.

We cannot determine K_C and B for DOPS separately from the x-ray data in this study. We have previously obtained both parameters for DOPC using a newly developed x-ray method that, for the first time, enables researchers to obtain both K_C and B for lipid bilayers that have values of K_C an order-of-magnitude larger than k_BT (Lyatskaya et al., 2001). Because it is not possible to measure P_{osm} accurately using that method, the present osmotic stress x-ray method will still be valuable for calibrating the value of P_{osm} that is required for the measured D-spacings. The present data have shown that the product K_CB is larger for DOPS than for DOPC. Although this larger value reduces the fluctuations that require the Caillé-type fluctuation analysis of x-ray data, these fluctuations are definitely present in the x-ray data in Fig. 2. Indeed, the magnitude of σ shown in Fig. 3 is even larger for DOPS than for DOPC at the same P_{osm}. Although the pressure due to these fluctuations is far smaller than the pressure from the electrostatic interactions in DOPS, this alone does not suppress the fluctuations, it merely makes the ratio σ/a smaller because the water spacing a is increased by the electrostatic repulsive interaction.

We thank Yufeng Liu for assistance with data collection at the Cornell High Energy Synchrotron Source and software programming. We also thank Sergey Bezrukov, Per Hansen, and Thomas Zemb for stimulating discussions.

We acknowledge use of the F1 and D1 stations of the Cornell High Energy Synchrotron Facility (National Science Foundation grant DMR-9311772). The Carnegie Mellon University authors and the initial data collection by Dr. Petrache were supported by National Institutes of Health grant GM44976 (JFN-PI).

REFERENCES

Andelman, D. 1995. Electrostatic Properties of Membranes: The Poisson-Boltzmann Theory, Vol. 1, 2nd Ed. R. Lipowsky and E. Sackmann, editors. Elsevier, Amsterdam, The Netherlands.

Bach, U. C., M. Baiersdorfer, G. Klock, M. Cattarazza, A. Post, and C. Koch-Brandt. 2001. Apoptotic cell debris and PS-containing lipid vesicles induce apolipoprotein J (clusterin) gene expression in vital fibroblasts. *Exp. Cell Res.* 265:11–20.

Barna, S. L., M. W. Tate, S. M. Gruner, and E. F. Eikenberry. 1999. Calibration procedures for charge-coupled device x-ray detectors. *Rev. Sci. Instr.* 70:2927–2934.

Bezrukov, S. M., P. R. Rand, I. Vodyanoy, and V. A. Parsegian. 1998. Lipid packing stress and polypeptide aggregation: alamethicin channel probed by proton titration of lipid charge. *Faraday Discuss.* 111:173–183.

Blankenberg, F. G., P. D. Katsikis, J. F. Tait, R. E. Davis, L. Naumovski, K. Ohtsuki, S. Kopiwoda, M. J. Abrams, M. Darkes, R. C. Robbins, H. T. Maecker, and H. W. Strauss. 1998. *In vivo* detection and imaging of phosphatidylserine expression during programmed cell death. *Proc. Natl. Acad. Sci. USA.* 95:6349–6354.

Botelho, A. V., N. J. Gibson, R. L. Thurmond, Y. Wang, and M. F. Brown. 2002. Conformational energetics of rhodopsin modulated by non-lamellar-forming lipids. *Biochemistry.* 41:6354–6368.

Brown, M. F. 1994. Modulation of rhodopsin function by properties of the membrane bilayer. *Chem. Phys. Lipids.* 74:159–180.

Browning, J. L., and J. Seelig. 1980. Bilayers of phosphatidylserine: a deuterium and phosphorus nuclear magnetic resonance study. *Biochemistry.* 19:1262–1270.

Cevc, G., A. Watts, and D. Marsh. 1981. Titration of the phase transition of phosphatidylserine bilayer membranes. Effects of pH, surface electrostatics, ion binding, and head-group hydration. *Biochemistry.* 20:4955–4965.

Cevc, G., M. Hauser, and A. A. Kornyshev. 1995. Effect of the interfacial structure on the hydration forces between laterally uniform surfaces. *Langmuir.* 11:3103–3110.

Cowley, A. C., N. L. Fuller, R. P. Rand, and V. A. Parsegian. 1978. Measurement of repulsive forces between charged phospholipid bilayers. *Biochemistry.* 17:3163–3168.

Daleke, D. L. 2002. Regulation of transbilayer plasma membrane phospholipid asymmetry. *J. Lipid Res.* 44:233–242.

Davies, M. A., W. Hubner, A. Blume, and R. Mendelsohn. 1992. Acyl chain conformational ordering in 1,2 dipalmitoylphosphatidylethanolamine. Integration of FT-IR and ^{2}H-NMR results. *Biophys. J.* 63:1059–1062.

de Kroon, A. I. P. M., J. W. Timmermans, J. A. Killian, and B. de Kruijff. 1990. The pH dependence of headgroup and acyl chain structure and dynamics of phosphatidylserine, studied by ^{2}N-NMR. *Chem. Phys. Lipids.* 54:33–42.

Demé, B., M. Dubois, T. Gulik-Krzywicki, and T. Zemb. 2002a. Giant collective fluctuations of charged membranes at the lamellar-to-vesicle unbinding transition. 1. Characterization of a new lipid morphology by SANS, SAXS, and electron microscopy. *Langmuir.* 18:997–1004.

Demé, B., M. Dubois, and T. Zemb. 2002b. Giant collective fluctuations of charged membranes at the lamellar-to-vesicle unbinding transition. 2. Equation of state in the absence of salt. *Langmuir.* 18:1005–1013.

Epand, R. M., C. Stevenson, R. Bruins, V. Schram, and M. Glaser. 1998. The chirality of phosphatidylserine and the activation of protein kinase C. *Biochemistry.* 37:12068–12073.

Evans, E. A., and V. A. Parsegian. 1986. Thermal-mechanical fluctuations enhance repulsion between biomolecular layers. *Proc. Natl. Acad. Sci. USA.* 83:7132–7136.

Fadok, V. A., D. R. Voelker, P. A. Campbell, J. J. Cohen, D. L. Bratton, and P. M. Hanson. 1992. Exposure of PS on the surface of apoptotic lymphocytes triggers specific recognition and reversal by macrophages. *J. Immunol.* 148:2207–2216.

Gally, H. U., W. Niederberger, and J. Seelig. 1975. Conformation and motion of the choline head group in bilayers of dipalmitoyl-3-*sn*-phosphatidylcholine. *Biochemistry.* 14:3647–3652.

Gawrisch, K., and L. L. Holte. 1996. NMR investigations of non-lamellar phase promoters in the lamellar phase state. *Chem. Phys. Lipids.* 81:105–116.

Gawrisch, K., W. Richter, A. Möps, P. Balgavý, K. Arnold, and G. Klose. 1985. The influence of water concentration on the structure of egg yolk phospholipid/water dispersions. *Studia Biophysica.* 108:5–10.

Gruner, S. M. 1985. Curvature hypothesis: does the intrinsic curvature determine biomembrane lipid composition? A role for non-bilayer lipids. *Proc. Natl. Acad. Sci. USA.* 82:3665–3669.

Hauser, H., F. Paltauf, and G. G. Shipley. 1982. Structure and thermotropic behavior of phosphatidylserine bilayer membranes. *Biochemistry.* 21:1061–1067.

Hoffmann, P. R., A. M. de Cathelineau, C. A. Ogden, Y. Leverrier, D. L. Bratton, D. L. Daleke, A. J. Ridley, V. A. Fadok, and P. M. Henson. 2001. Phosphatidylserine (PS) induces PS receptor-mediated macropinocytosis and promotes clearance of apoptotic cells. *J. Cell Biol.* 155:649–659.

Holte, L. L., S. A. Peter, T. M. Sinnwell, and K. Gawrisch. 1995. ^{2}H nuclear magnetic resonance order parameter profiles suggest a change of

molecular shape for phosphocholines containing a polyunsaturated acyl chain. *Biophys. J.* 68:2396–2403.

Huster, D., K. Arnold, and K. Gawrisch. 1998. Influence of docosahexaenoic acid and cholesterol on lateral lipid organization in phospholipid mixtures. *Biochemistry.* 37:17299–17308.

Johnson, J. E., M. L. Zimmerman, D. L. Daleke, and A. C. Newton. 1998. Lipid structure and not membrane structure is the major determinant in the regulation of protein kinase C by phosphatidylserine. *Biochemistry.* 37:12020–12025.

Katsaras, J. 1998. Adsorbed to a rigid substrate, dimyristoylphosphatidylcholine multibilayers attain full hydration in all mesophases. *Biophys. J.* 75:2157–2162.

Katsaras, J., and M. J. Watson. 2000. Sample cell capable of 100% relative humidity suitable for x-ray diffraction of aligned lipid multibilayers. *Rev. Sci. Instrum.* 71:1737–1739.

Kim, H.-Y., A. Mohammed, L. Audrey, and L. Edsall. 2000. Inhibition of neuronal apoptosis by docosahexaenoic acid (22:6n3): role of PS in antiapoptotic effect. *J. Biol. Chem.* 275:35215–35223.

Koenig, B. W., H. H. Strey, and K. Gawrisch. 1997. Membrane lateral compressibility determined by NMR and x-ray diffraction: effect of acyl chain polyunsaturation. *Biophys. J.* 73:1954–1966.

Lewis, R. N. A. H., and R. N. McElhaney. 2000. Calorimetric and spectroscopic studies of the thermotropic phase behavior of lipid bilayer membranes composed of a homologous series of linear saturated phosphatidylserines. *Biophys. J.* 79:2043–2055.

Loosley-Milman, M. E., R. P. Rand, and V. A. Parsegian. 1982. Effects of monovalent ion binding and screening or measured electrostatic forces between charged phospholipid bilayers. *Biophys. J.* 40:221–232.

Lyatskaya, Y., Y. F. Liu, S. Tristram-Nagle, J. Katsaras, and J. F. Nagle. 2001. Method for obtaining structure and interactions from oriented lipid bilayers. *Phys. Rev. E.* 63:011907.

MacDonald, R. C., S. A. Simon, and E. Baer. 1976. Ionic influences on the phase transition of dipalmitoylphosphatidylserine. *Biochemistry.* 15:885–891.

Manno, S., Y. Takakuwa, and N. Mohandas. 2002. Identification of a functional role for the lipid asymmetry in biological membranes: phosphatidylserine-skeletal protein interactions modulate membrane stability. *Proc. Natl. Acad. Sci. USA.* 99:1943–1948.

Marsh, D. 1989. Water absorption isotherms and hydration forces for lysolipids and diacyl phospholipids. *Biophys. J.* 55:1093–1100.

Marsh, D., A. Watts, and I. C. P. Smith. 1983. Dynamic structure and phase behavior of dimyristoylphophatidylethanolamine bilayers studied by deuterium nuclear magnetic resonance. *Biochemistry.* 22: 3023–3026.

Mason, J. T., and T. J. O'Leary. 1990. Effects of headgroup methylation and acyl chain length on the volume of melting of phosphatidylethanolamines. *Biophys. J.* 58:277–281.

McIntosh, T. J. 1980. Differences in hydrocarbon chain tilt between hydrated phosphatidylethanolamine and phosphatidylcholine bilayer. A molecular packing model. *Biophys. J.* 29:237–245.

McIntosh, T. J., and S. A. Simon. 1986. Area per molecule and distribution of water in fully hydrated dilauroylphosphatidylethanolamine bilayers. *Biochemistry.* 25:4948–4952.

McIntosh, T. J., and S. A. Simon. 1996. Adhesion between phosphatidylethanolamine bilayers. *Langmuir.* 12:1622–1630.

Mukhopadhyay, P. L. Monticelli, and D. P. Tieleman. 2004. Molecular dynamics simulation of a palmitoyl-oleoyl phosphatidylserine bilayer with Na^+ counterions and NaCl. *Biophys. J.* 86-3:1601–1610.

Nagle, J. F. 1976. Theory of lipid monolayer and bilayer phase transition: effect of headgroup interactions. *J. Membr. Biol.* 27:233–250.

Nagle, J. F., and S. Tristram-Nagle. 2000. Structure of lipid bilayers. *Biochim. Biophys. Acta.* 1469:159–195.

Nagle, J. F., and M. C. Wiener. 1989. Relations for lipid bilayers: connection of electron density profiles to other structural quantities. *Biophys. J.* 55:309–313.

Nagle, J. F., R. Zhang, S. Tristram-Nagle, W.-J. Sun, H. I. Petrache, and R. M. Suter. 1996. X-ray structure determination of fully hydrated L_α phase DPPC bilayers. *Biophys. J.* 70:1419–1431.

Pandit, S. A., and M. L. Berkowitz. 2002. Molecular dynamics simulation of dipalmitoylphosphatidylserine bilayer with Na^+ counterions. *Biophys. J.* 82:1818–1827.

Parsegian, V. A., N. Fuller, and R. P. Rand. 1979. Measured work of deformation and repulsion of lecithin bilayers. *Proc. Natl. Acad. Sci. USA.* 76:2750–2754.

Parsegian, V. A., and R. P. Rand. 1983. Membrane interaction and deformation. *Ann. NY Acad. Sci.* 416:1–12.

Petrache, H. I., S. W. Dodd, and M. F. Brown. 2000. Area per lipid and acyl length distributions in fluid phosphatidylcholines determined by ^{2}H-NMR spectroscopy. *Biophys. J.* 79:3172–3192.

Petrache, H. I., N. Gouliev, S. Tristram-Nagle, R. Zhang, R. M. Suter, and J. F. Nagle. 1998a. Interbilayer interactions from high-resolution x-ray scattering. *Phys. Rev. E.* 57:7014–7024.

Petrache, H. I., S. Tristram-Nagle, and J. F. Nagle. 1998b. Fluid phase structure of EPC and DMPC bilayers. *Chem. Phys. Lipids.* 95:83–94.

Podgornik, R., and V. A. Parsegian. 1992. Thermal-mechanical fluctuations of fluid membranes in confined geometries: the case of soft confinement. *Langmuir.* 8:557–562.

Rand, R. P., N. Fuller, V. A. Parsegian, and D. C. Rau. 1988. Variation in hydration forces between neutral lipid bilayers: evidence for hydration attraction. *Biochemistry.* 27:7711–7722.

Rand, R. P., and V. A. Parsegian. 1989. Hydration forces between phospholipid bilayers. *Biochim. Biophys. Acta.* 988:351–376.

Rawicz, W., K. C. Olbrich, T. McIntosh, D. Needham, and E. Evans. 2000. Effect of chain length and unsaturation on elasticity of lipid bilayers. *Biophys. J.* 79:328–339.

Separovic, F., and K. Gawrisch. 1996. Effect of unsaturation on the chain order of phosphatidylcholines in a dioleoylphosphatidylethanolamine matrix. *Biophys. J.* 71:274–282.

Simon, S. A., C. A. Fink, A. K. Kenworthy, and T. J. McIntosh. 1991. The hydration pressure between lipid bilayers. Comparison of measurements using x-ray diffraction and calorimetry. *Biophys. J.* 59:538–546.

Slater, S. J., M. B. Kelly, F. J. Taddeo, C. Ho, E. Rubin, and C. D. Stubbs. 1994. The modulation of protein kinase C activity by membrane lipid bilayer structure. *J. Biol. Chem.* 269:4866–4871.

Sun, W.-J., S. Tristram-Nagle, R. M. Suter, and J. F. Nagle. 1996. Structure of gel phase saturated lecithin bilayers: temperature and chain length dependence. *Biophys. J.* 71:885–891.

Takai, Y., A. Kishimoto, Y. Iwasa, Y. Kawahara, T. Mori, and Y. Nishizuka. 1979. Calcium-dependent activation of a multifunctional protein kinase by membrane phospholipids. *J. Biol. Chem.* 254:3692–3695.

Tardieu, A., V. Luzzati, and F. C. Freeman. 1973. Structure and polymorphism of the hydrocarbon chains of lipids: a study of lecithin-water phases. *J. Mol. Biol.* 75:711–733.

Tate, M. W., E. F. Eikenberry, S. L. Barna, M. E. Wall, J. L. Lowrance, and S. M. Gruner. 1995. A large-format high-resolution area x-ray detector based on a fiber-optically bonded charge-coupled device (CCD). *J. Appl. Crystallogr.* 28:196–205.

Thurmond, R. L., S. W. Dodd, and M. F. Brown. 1991. Molecular areas of phospholipids as determined by ^{2}H-NMR spectroscopy. *Biophys. J.* 59:108–113.

Tristram-Nagle, S., Y. Liu, J. Legleiter, and J. F. Nagle. 2002. Structure of gel phase DMPC determined by x-ray diffraction. *Biophys. J.* 83:3324–3335.

Tristram-Nagle, S., H. I. Petrache, and J. F. Nagle. 1998. Structure and interactions of fully hydrated dioleoylphosphatidylcholine bilayers. *Biophys. J.* 75:917–925.

Tristram-Nagle, S., R. Zhang, R. M. Suter, C. R. Worthington, W.-J. Sun, and J. F. Nagle. 1993. Measurement of chain tilt angle in fully hydrated bilayers of gel phase lecithins. *Biophys. J.* 64:1097–1109.

Tsvetkova, N. M., I. Horváth, Z. Török, W. F. Wolkers, Z. Balogi, N. Shigapova, L. M. Crowe, F. Tablin, E. Vierling, J. H. Crowe, and L. Wigh. 2002. Small heat-shock proteins regulate membrane lipid polymorphism. *Proc. Natl. Acad. Sci. USA.* 99:13504–13509.

Volke, F., S. Eisenbläter, J. Galle, and G. Klose. 1994a. Dynamic properties of water at phosphatidylcholine lipid-bilayer surfaces as seen by deuterium and pulsed field gradient proton NMR. *Chem. Phys. Lipids.* 70:121–131.

Volke, F., S. Eisenbläter, and G. Klose. 1994b. Hydration force parameters of phosphatidylcholine lipid bilayers as determined from ^{2}H-NMR studies of deuterated water. *Biophys. J.* 67:1882–1887.

Weinreb, G. E., K. Mukhopadhyay, R. Majumder, and B. R. Lentz. 2003. Cooperative role of factor V-a and phosphatidylserine-containing membranes as cofactors in prothrombin activation. *J. Biol. Chem.* 278:5679–5684.

Wiener, M. C., S. Tristram-Nagle, D. A. Wilkinson, L. E. Campbell, and J. F. Nagle. 1988. Specific volumes of lipids in fully hydrated bilayer dispersions. *Biochim. Biophys. Acta.* 938:135–142.

Wilkinson, D. A., and J. F. Nagle. 1981. Dilatometry and calorimetry of saturated phosphatidylethanolamines. *Biochemistry.* 20:187–192.

Yang, L., and M. Glaser. 1995. Membrane domains containing phosphatidylserine and substrate can be important for the activation of protein kinase C. *Biochemistry.* 34:1500–1506.

Yang, L., and M. Glaser. 1996. Formation of membrane domains during the activation of protein kinase C. *Biochemistry.* 35:13966–13974.

Zhang, R., R. M. Suter, and J. F. Nagle. 1994. Theory of the structure factor of lipid bilayers. *Phys. Rev. E.* 50:5047–5060.